ChemComm

Accepted Manuscript

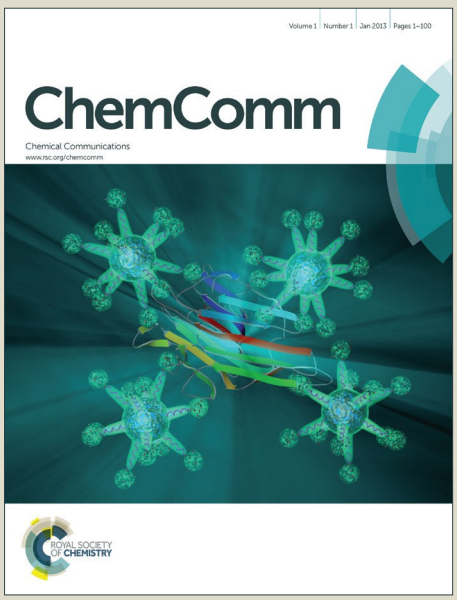

ROYAL SOCIETY OF CHEMISTRY

www.rsc.org/chemcomm

ChemComm

COMMUNICATION

Enhancement of electrochemical properties by polysulfide trap in graphene-coated sulfur cathode on patterned current collector†

Seung-Ho Yu,‡[a,b] Bora Lee,‡[c] Sinho Choi,[d] Soojin Park,[d] Byung Hee Hong*[,c] and Yung-Eun Sung*[,a,b]

Received 00th January 20xx,
Accepted 00th January 20xx

DOI: 10.1039/x0xx00000x

www.rsc.org/

A sulfur cathode on a honeycomb-shape-patterned Al current collector was prepared and successfully sealed using triple-layered graphene. Graphene layers on the sulfur cathode well confined the dissolved polysulfide in the electrode, leading to significantly enhanced electrochemical properties including cycle retention and Coulombic efficiency.

Lithium-sulfur (Li-S) rechargeable batteries have been considered a promising next-generation energy system owing to their high theoretical energy density of 2600 Wh kg^{-1}, low cost, and nontoxicity.[1-3] However, their practical use is hampered by several issues such as low sulfur utilization, resulting from the low intrinsic conductivity of sulfur, and poor cycle stability.[4] Among these issues, polysulfide dissolution in the organic electrolyte is the most critical problem that should be overcome, and it is responsible for the polysulfide shuttle phenomenon, low Coulombic efficiency, and active-material loss.[5,6]

Various approaches have been proposed to reduce the polysulfide dissolution in the electrolyte.[7-13] The most common strategy is confining sulfur in pores in carbonaceous materials. In 2009, Nazar's group first demonstrated this strategy by using sulfur-infiltrated ordered mesoporous carbon (CMK-3).[7] In addition, many microporous carbonaceous materials have been developed to confine metastable small sulfur molecules, and they have shown significantly enhanced cycle stability.[8-10] However, the low sulfur content in microporous carbon/sulfur composites and relatively low reaction voltage of small sulfur molecules decrease the total energy density. Another effective way is to introduce an interlayer between the sulfur cathode and separator.[14-19] Manthiram's group showed that microporous carbon paper included between the cathode and separator improved the active-material utilization by localizing the soluble polysulfide.[14] An alternative approach is to control the polysulfide solubility by modifying some components in the organic electrolyte or replacing the organic electrolyte with others such as ionic liquids or solid-state electrolytes.[20-23] A solid-state electrolyte can completely prevent polysulfide dissolution, but the poor lithium-ion conductivity remains another hurdle.[22,23]

Recently, graphene has been implemented as a part of electrode materials for lithium ion batteries and lithium sulfur batteries due to its unique physical and chemical properties, improving the electrochemical performance of cells significantly.[24-28] Herein, a graphene-coated sulfur cathode was fabricated by transferring graphene prepared by chemical vapor deposition onto a sulfur cathode on a pattered Al current collector. This resulted in significantly enhanced cyclic stability and Coulombic efficiency during 100 cycles because triple-layered graphene effectively confined the polysulfide in the sulfur cathode. In addition, the low-potential barrier of the graphene-coated sulfur cathode in the charge and discharge profiles resulted from the high concentration of polysulfide in the electrode, which was achieved by the successful polysulfide trap.

Scheme 1 schematically shows the preparation of the graphene-coated sulfur cathode on a honeycomb-shape-pattered Al current collector (GCSC). In order to coat the graphene onto a sulfur cathode effectively, the surface of the sulfur cathode should be rather flat. An Al current collector was etched on the cathode to reduce the height difference between the top of sulfur and Al current collector after sulfur loading. In particular, the honeycomb-patterned Al current collector prepared using the reactive-ion etching process enables the

[a] *Center for Nanoparticle Research, Institute for Basic Science (IBS), Seoul 151-742, Republic of Korea*
[b] *School of Chemical and Biological Engineering, Seoul National University, Seoul 151-742, Republic of Korea*
[c] *Department of Chemistry, College of Natural Sciences, Seoul National University, Daehack-dong, Gwanak-gu, Seoul, 151-747, Republic of Korea*
[d] *Department of Energy Engineering, School of Energy and Chemical Engineering, Ulsan National Institute of Science and Technology (UNIST), Ulsan 689-798, Republic of Korea.*
‡ *The authors contribute equally to this work.*
† Electronic Supplementary Information (ESI) available: [details of any supplementary information available should be included here]. See DOI: 10.1039/x0xx00000x

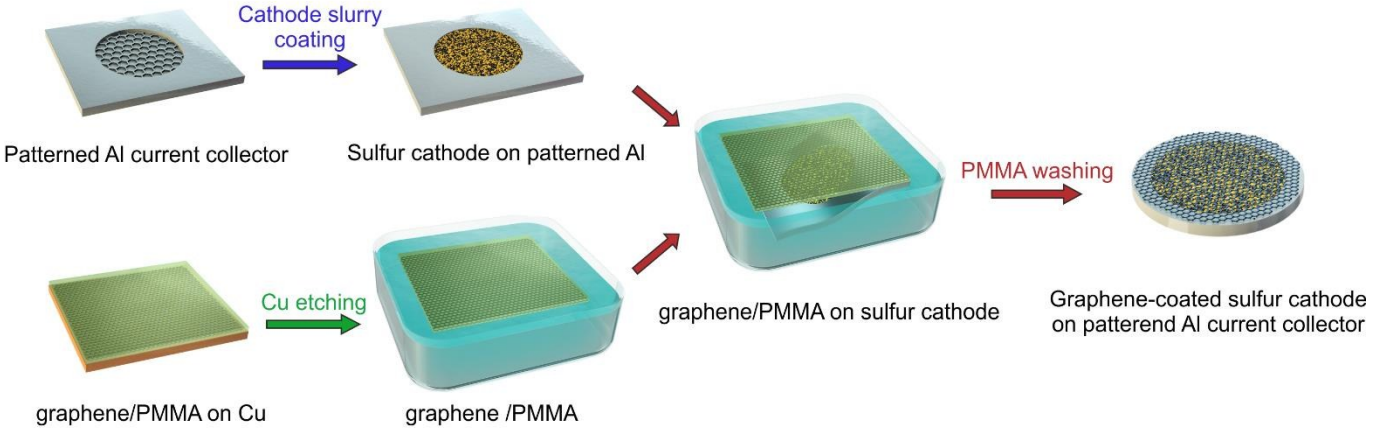

Scheme 1 Schematic representation of GCSC preparation.

maximum adhesion between the current collector and active materials, and provides an efficient pathway for electron transport.[29,30] The top-view field-emission scanning electron microscopy (SEM) image shows that the Al current collector is well patterned with a honeycomb shape over a large area (Fig. 1a and Fig. S1). The width of each honeycomb is about 50 μm (Fig. 1b). The etched region on the Al current collector is filled with a mixture of sulfur, conductive carbon, and binder (Fig. 1c).

Previously, many interlayers had been introduced in the Li-S battery system, but they were simply placed between the cathode and separator. Consequently, some dissolved polysulfide could migrate out near the electrode through the gap between the cathode and interlayers. In order to avoid a gap through which polysulfide can migrate out from the electrode, the Al current collector around the cathode was kept unpatterned to adhere with the graphene layer. The trilayer graphene fully covered Al current collector (see Scheme S1 for cross-sectional illustration of graphene-coated sulfur cathode on patterned Al current collector). Single-layer graphene deposited on a copper foil by using the chemical vapor deposition method was coated with poly(methyl methacrylate) (PMMA), following which the copper foil was dissolved out. Optical microscopy image and atomic force microscopy (AFM) images, and Raman spectra of single-layer graphene were shown in Fig. S2. Optical microscopy and AFM images clearly show the single-layer graphene sheet. In particular, the large 2D/G peak ratio (2.73 ± 0.4) and the negligible D peak intensities in Raman spectra of graphene transferred onto Si/SiO_2 substrates indicate that the graphene film is a high-quality single layer.[31] The PMMA-graphene single layer was transferred onto another graphene layer. This process was repeated to form triple-layered graphene, which was transferred to the sulfur electrode on a pattered Al foil (Fig. 1d). The graphene layers fully coated the sulfur cathode on the patterned Al current collector and adhered to the unpatterned Al current collector around the sulfur cathode to better trap the polysulfide in the electrode. Figs. 1e-h show the SEM image and

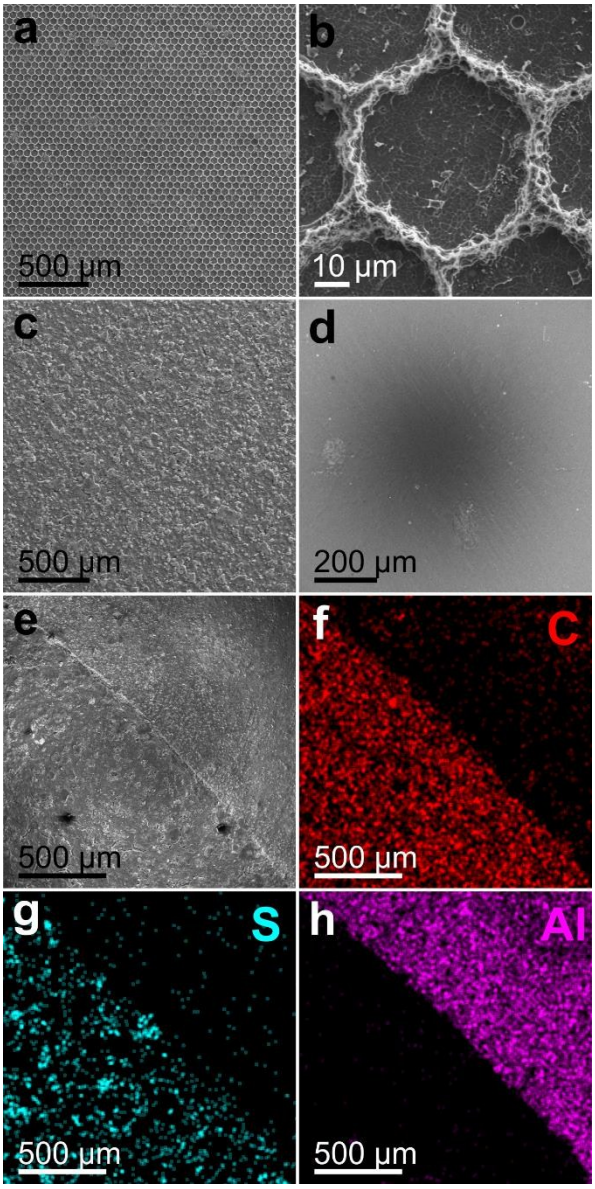

Fig. 1 Top-view SEM images of (a), (b) patterned Al current collector, (c) sulfur cathode on patterned Al current collector, and (d) GCSC. (e) Top-view SEM image and (f)-(h) corresponding EDX mapping of sulfur cathode on patterned Al current collector at the boundary line of patterning for C, S and Al, respectively.

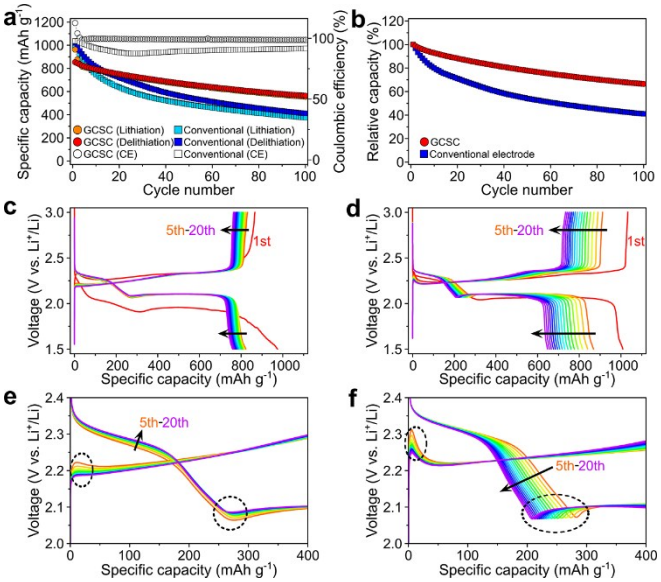

Fig. 2 (a) Cycle performance and Coulombic efficiency of GCSC and conventional electrode for comparison at 0.2 C. (b) Relative capacity of GCSC and conventional electrode on cycling. Voltage profiles of (c) GCSC and (d) conventional electrode at the first cycle and fifth to twentieth cycle. Enlarged voltage profiles of (e) GCSC and (f) conventional electrode.

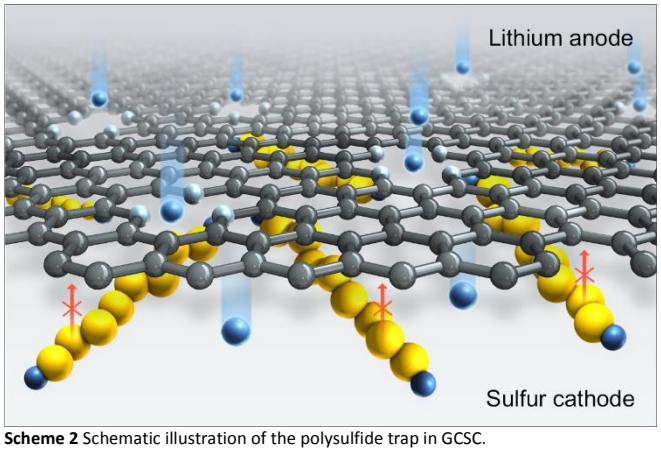

Scheme 2 Schematic illustration of the polysulfide trap in GCSC.

corresponding energy-dispersive X-ray spectroscopy (EDX) mappings of the fabricated sulfur cathode on a patterned Al current collector at the boundary line before graphene coating. The boundary line between the sulfur cathodes on patterned and unpatterned Al is clearly observed in both the SEM image and EDX mappings, which indicates that the sulfur cathode material is well filled only on the patterned empty space.

To evaluate the electrochemical behavior of GCSC, a galvanostatic charge and discharge test was conducted with a 2032-type coin cell. A sulfur cathode of the same composition without the patterning of the Al current collector or a graphene layer coating (conventional electrode) was also analyzed for comparison (see Fig. S3 for electrochemical performance of sulfur cathode on patterned Al current collector without graphene coating for comparison). The PMMA layer supporting the graphene layers was washed out using the electrolyte. Fig. 2a presents the cycle performance and Columbic efficiency of GCSC and the conventional electrode at a rate of 0.2 C (1 C =1672 mAh g^{-1}). The delithiation capacity of the conventional electrode decreased rapidly during 100 cycles and reached 423 mAh g^{-1} at the 100th cycle. The Coulombic efficiency of the conventional electrode is 90.3% on average during 100 cycles, and the lowest value is 87.4% at the 28th cycle. The polysulfide shuttle reaction, which is caused by polysulfide dissolution, the migration of polysulfide in the electrolyte, and the reaction between polysulfide and lithium anode, is considered the major reason for the low Coulombic efficiency of the conventional electrode. The GCSC exhibits significantly enhanced electrochemical performance in terms of cyclic stability and Coulombic efficiency during 100 cycles. The Coulombic efficiency of GCSC is 99.2% on average during 100 cycles. The delithiation capacity of GCSC at the 100th cycle is 576 mAh g^{-1}. The improved cycle stability of GCSC is more clearly seen in cycle retention during 100 cycles (Fig. 2b), which shows that the cycle retentions of GCSC and the conventional electrode are 66.5% and 41.0%, respectively. Figs. 2c and d show the voltage profiles of GCSC and the conventional electrode from the 5th to 20th cycle and the initial cycle, respectively. Both GCSC and the conventional electrode show two clear lithiation plateaus of sulfur in the organic electrolyte. The first lithiation voltage of GCSC is relatively lower than that of the conventional electrode or other reported sulfur cathodes in organic solvents, which might be due to the activation process for the first lithium-ion transport though the defects of graphene layers. According to discharge voltage profiles during the 5th to 20th cycle, the capacity delivered from the upper plateau of GCSC was maintained, whereas that of the conventional electrode decreased on cycling. Potential barriers are observed in charge and discharge profiles in both electrodes, as circled in Figs. 2e and f. The potential barrier during the discharge process at the lower plateau is related to the phase nucleation of soluble polysulfide to insoluble lithium sulfide. In addition, the potential barrier at the early stage of the charge process is due to a slow charge-transfer process between the electrolyte and lithium sulfide.[32] Both potential barriers during charge and discharge decrease as the concentration of polysulfide increases.[32] Therefore, the potential barriers keep decreasing with subsequent cycling, as can be seen in Figs. 2e and f. It is worthwhile to comment that GCSC has much smaller potential barriers than those of the conventional electrode, which indicates that GCSC distinctly traps polysulfides in the electrode. The significant decrease in the potential barrier can also be seen in many interlayer-introduced sulfur cathodes.[13-18] The better kinetics of GCSC compared to conventional electrode is also observed in cyclic voltammograms (Fig. S4). Scheme 2 illustrates the polysulfide trap in GCSC. The soluble polysulfides cannot migrate out through the graphene layers owing to their large size, but lithium ions can transfer through the defects of graphene layer.

In summary, a graphene-coated sulfur cathode was successfully prepared by patterning an Al current collector with a honeycomb shape, loading the sulfur with a conductive agent and binder, and coating the top of electrode with graphene layers fabricated using chemical vapor deposition. The graphene-coated sulfur cathode showed significantly improved cyclic stability with Coulombic efficiency (99.2% on average)

during 100 cycles compared to conventional sulfur electrode. This improvement in electrochemical property is due to the prevention of polysulfide migration from the cathode to the electrolyte. A significant decrease in the potential barriers in the charge and discharge profiles is also caused by the effective confinement of polysulfide.

Thank A. Jin, K. R. Kim and K. Kang for experimental help and discussions for electrochemical analysis. This research was supported by Basic Science Research Program through the National Research Foundation of Korea (NRF) funded by the Ministry of Education (2015R1A6A3A03020354). Y. –E. Sung acknowledges the financial support by IBS-R006-G1.

Notes and references

1 P. G. Bruce, S. A. Freunberger, L. J. Hardwick and J. –M. Tarascon, *Nat. Mat.*, 2012, **11**, 19.
2 Y. –X. Yin, S. Xin, Y. –G. Guo and L. –J. Wan, *Angew. Chem. Int. Ed*., 2013, **52**, 13186.
3 A. Manthiram, Y. Fu, S. –H. Chung, C. Zu and Y. –S. Su, *Chem. Rev*., 2014, **114**, 11751.
4 S. Urbonaite, T. Poux and P. Novák, *Adv. Energy Mater*., 2015, **5**, 1500118.
5 M. Barghamadi, A. S. Best, A. I. Bhatt, A. F. Hollenkamp, M. Musameh, R. J. Rees and T. Rüther, *Energy Environ. Sci.*, 2014, **7**, 3902.
6 K. R. Kim, S. –H. Yu and Y. –E. Sung, *Chem. Comm.*, 2016, **52**, 1198.
7 X. Ji, K. T. Lee and L. F. Nazar, *Nat. Mat.*, 2009, **8**, 500.
8 S. Xin, L. Gu, N. –H. Zhao, Y. –X. Yin, L. –J. Zhou, Y. –G. Guo and L. –J. Wan, *J. Am. Chem. Soc.*, 2012, **134**, 18510.
9 Y. Xu, Y. Wen, Y. Zhu, K. Gaskell. K. A. Cychosz, B. Eichhorn, K. Xu and C. Wang, *Adv. Funct. Mater.*, 2015, **25**, 4312.
10 Z. Li and L. Yin, *ACS Appl. Mater. Interfaces*, 2015, **7**, 4029.
11 Z. Li, Y. Jiang, L. Yuan, Z. Yi, C. Wu, Y. Liu, P. Strasser and Y. Huang, *ACS Nano*, 2014, **8**, 9295.
12 W. Zhou, Y. Yu, H. Chen, F. J. DiSalvo and H. D. Abruña, *J. Am. Chem. Soc.*, 2013, **135**, 16736.
13 W. J. Chung, J. J. Griebel, E. T. Kim, H. Yoon, A. G. Simmonds, H. J. Ji, P. T. Dirlam, R. S. Glass, J. J. Wie, N. A. Nguyen, B. W. Guralnick, J. Park, Á. Somogyi, P. Theato, M. E. Mackay, Y. –E. Sung, K. Char and J. Pyun, *Nat. Chem.*, 2013, **5**, 518.
14 Y. –S. Su and A. Manthiram, *Nat. Comm.*, 2012, **3**, 1166.
15 Z. Xiao, Z. Yang, L. Wang, H. Nie, M. Zhong, Q. Lai, X. Xu, L. Zhang and S. Huang, *Adv. Mater.*, 2015, **27**, 2891.
16 G. Zhou, S. Pei, L. Li, D. –W. Wang, S. Wang, K. Huang, L. –C. Yin, F. Li and H. –M. Cheng, *Adv. Mater.*, 2014, **26**, 625.
17 G. Ma, Z. Wen, Q. Wang, C. Shen, P. Peng, J. Jin and X. Wu, *J. Power Sources*, 2015, **273**, 511.
18 J. Song, Z. Yu, T. Xu, S. Chen, H. Sohn, M. Regula and D. Wang, *J. Mater. Chem A*, 2014, **2**, 8623.
19 S. –H. Chung and A. Manthiram, *J. Phys. Chem. Lett.*, 2014, **5**, 1978.
20 M. Cuisinier, P. –E. Cabelguen, B. D. Adams, A. Garsuch, M. Balasubramanian and L. F. Nazar, *Energy Environ. Sci.*, 2014, **7**, 2697.
21 L. Suo, Y. –S. Hu, H. Li, M. Armand and L. Chen, *Nat. Comm.*, 2013, **4**, 1481.
22 M. Nagao, A. Hayashi and M. Tatsumisago, *Electrochem. Comm.*, 2012, **22**, 177.
23 Z. Lin, Z. Liu, N. J. Dudney and C. Liang, *ACS Nano*, 2013, **7**, 2829.
24 X. Zhou, X. Liu, Y. Wu, Y. Liu, Z. Dai and J. Bao, *J. Phys. Chem. C*, 2014, **118**, 23527.
25 Y. Du, X. Zhu, X. Zhou, L. Hu, Z. Dai and J. Bao, *J. Mater. Chem. A*, 2015, **3**, 6787.
26 S. –H. Yu, D. E. Conte, S. Baek, D. –C. Lee, S. –K. Park, K. J. Lee, Y. Piao, Y. –E. Sung and N. Pinna, *Adv. Funct. Mater.*, 2013, **23**, 4293.
27 B. Quan, S. –H. Yu, D. Y. Chung, A. Jin, J. H. Park, Y. –E. Sung and Y. Piao, *Sci. Rep.*, 2014, **4**, 5639.
28 H. Wang, Y. Yang, Y. Liang, J. T. Robinson, Y. Li, A. Jackson, Y. Cui and H. Dai, *Nano Lett.*, 2011, **11**, 2644.
29 M. –H. Park, M. Noh, S. Lee, M. Ko, S. Chae, S. Sim, S. Choi, H. Kim, H. Nam, S. Park and J. Cho, *Nano Lett.*, 2014, **14**, 4083.
30 S. Choi, T. –H. Kim, J. –In. Lee, J. Kim, H. –K. Song and S. Park, *ChemSusChem*, 2014, **7**, 3483.
31 A. C. Ferrari, J. C. Meyer, V. Scardaci, C. Casiraghi, M. Lazzeri, F. Mauri, S. Piscanec, D. Jiang, K. S. Novoselov, S. Roth and A. K. Geim, *Phys. Rev. Lett.*, 2006, **97**, 187401.
32 Y. Son, J. –S. Lee, Y. Son, J. –H. Jang and J. Cho, *Adv. Energy Mater.*, 2015, **5**, 1500110.